NMR Study of the Inhibition of Pepsin by Glyoxal Inhibitors: Mechanism of Tetrahedral Intermediate Stabilization by the Aspartyl Proteases†

Sonya Cosgrove, Louis Rogers, Chandralal M. Hewage, and J. Paul G. Malthouse*

UCD School of Biomolecular and Biomedical Science, Centre for Synthesis and Chemical Biology, Conway Institute, University College Dublin, Belfield, Dublin 4, Ireland

Received May 23, 2007; Revised Manuscript Received July 25, 2007

ABSTRACT: Z-Ala-Ala-Phe-glyoxal (where Z is benzyloxycarbonyl) has been shown to be a competitive inhibitor of pepsin with a $K_i = 89 \pm 24$ nM at pH 2.0 and 25 °C. Both the ketone carbon ($R^{13}COCHO$) and the aldehyde carbon ($RCO^{13}CHO$) of the glyoxal group of Z-Ala-Ala-Phe-glyoxal have been ^{13}C-enriched. Using ^{13}C NMR, it has been shown that when the inhibitor is bound to pepsin, the glyoxal keto and aldehyde carbons give signals at 98.8 and 90.9 ppm, respectively. This demonstrates that pepsin binds and preferentially stabilizes the fully hydrated form of the glyoxal inhibitor Z-Ala-Ala-Phe-glyoxal. From ^{13}C NMR pH studies with glyoxal inhibitor, we obtain no evidence for its hemiketal or hemiacetal hydroxyl groups ionizing to give oxyanions. We conclude that if an oxyanion is formed its pK_a must be >8.0. Using ^1H NMR, we observe four hydrogen bonds in free pepsin and in pepsin/Z-Ala-Ala-Phe-glyoxal complexes. In the pepsin/pepstatin complex an additional hydrogen bond is formed. We examine the effect of pH on hydrogen bond formation, but we do not find any evidence for low-barrier hydrogen bond formation in the inhibitor complexes. We conclude that the primary role of hydrogen bonding to catalytic tetrahedral intermediates in the aspartyl proteases is to correctly orientate the tetrahedral intermediate for catalysis.

Specific substrate-derived glyoxal inhibitors of proteases have been synthesized (*1*) and shown to be potent reversible inhibitors of chymotrypsin (*2*−*5*), subtilisin (*6*), papain (*7*), cathepsin B (*5*, *8*), cathepsin L (*8*), cathepsin S (*9*), and the proteasome (*10*). In addition, there has been a single report in the literature of the modest inhibition of HIV-1 aspartyl protease by peptides containing an N-terminal glyoxylyl function (CHO−CO−NH−) (*11*).

It is the formation and or breakdown of a tetrahedral intermediate which is thought to be the rate-limiting step in catalysis by proteases with natural substrates. Therefore, the proteases are thought to achieve their remarkable catalytic efficiency by transition-state stabilization of tetrahedral intermediate formation and or breakdown. Therefore, inhibitors which mimic these tetrahedral intermediates are often tightly bound and act as transition-state analogues, as articulated originally by Pauling (*12*) and demonstrated experimentally for the first time by Wolfenden (*13*).

Our recent studies on chymotrypsin and subtilisin with substrate-derived glyoxal inhibitors have shown that they form tetrahedral adducts with the active site serine hydroxyl group of both enzymes and that both enzymes provide significant oxyanion stabilization (*2*, *3*, *6*). In glyoxal inhibitors the aldehyde carbon is usually fully hydrated in aqueous solution. However, the glyoxal keto carbonyl carbon is usually only ∼70% hydrated in aqueous solution (*2*, *3*, *6*).

$$RCOCH(OH)_2 + H_2O = RC(OH)_2CH(OH)_2$$

In peptide-derived glyoxal inhibitors it is the glyoxal keto carbon which is equivalent to the peptide carbonyl of a substrate. Therefore, it is the glyoxal keto carbon ($RCOCH(OH)_2$) which reacts with the active site serine hydroxyl group to give the tetrahedral adduct with the serine proteases.

Catalysis by the aspartyl proteases is thought to involve binding of a peptide substrate followed by addition of water to the substrate peptide carbonyl carbon to form a tetrahedral intermediate (*14*, *15*). Therefore, if pepsin utilizes ground-state destabilization for catalysis, it would be expected to bind the keto form ($RCOCH(OH)_2$) of the glyoxal inhibitor, while if pepsin utilizes transition-state stabilization, it is the fully hydrated glyoxal inhibitor ($RC(OH)_2CH(OH)_2$) which will be optimally bound. However, there are four possible hydration states of glyoxal inhibitors, one fully hydrated form ($RC(OH)_2CH(OH)_2$), two monohydrated forms ($RCOCH(OH)_2$ and $RC(OH)_2CHO$), and one fully dehydrated form (RCOCHO). In the present study, we show that glyoxal inhibitors are potent inhibitors of pepsin and we identify which of the four possible hydration forms of the glyoxal inhibitor Z-Ala-Ala-Phe-glyoxal[1] are bound by pepsin.

We use ^1H NMR to observe H-bonded protons in free pepsin and in pepsin−inhibitor complexes formed with pepstatin and Z-Ala-Ala-Phe-glyoxal. Our results are sig-

† This work was supported by Basic Research Grant SC/2003/031 from Enterprise Ireland and grants from the Programme for Research in Third-Level Institutions (PRTLI-3) and the Irish Research Council for Science, Engineering and Technology (IRCSET). Grant 055637/Z/98 from the Wellcome Trust was used to purchase the NMR spectrometer used in these studies.

* To whom correspondence should be addressed. Phone: +353 1 7166872. Fax: +353 1 2837211. E-mail: J.Paul.G.Malthouse@ucd.ie.

[1] Abbreviation: Z, benzyloxycarbonyl.

10.1021/bi701000k CCC: $37.00
Published on Web 09/07/2007

nificantly different from those of earlier studies on β-secretases (*16*) and endathiapepsin (*17*, *18*). We discuss the role of hydrogen bonding in stabilizing *gem*-diols formed during catalysis and on binding inhibitors.

EXPERIMENTAL PROCEDURES

Materials. L-[1-^{13}C]Phenylalanine (99 atom %) was obtained from Cambridge Isotope Laboratories, Inc. (50, Frontage Rd., Andover, MA 01810-5413) and from CDN Isotopes (88 Leacock St., Pointe-Claire, Quebec, Canada). All other chemicals used were obtained from Aldrich Chemical Co., Gillingham, Dorset, U.K.

Synthesis of Z-Ala-Ala-Phe- and Z-Ala-Ala-[1-^{13}C]Phe. A 0.5 g (3 mmol) portion of L-phenylalanine or L-[1-^{13}C]-phenylalanine was added to 25 mL of methanol and the resulting mixure cooled to 0 °C in an ice bath. Hydrogen chloride gas was bubbled through the solution for 1 h, and the reaction was stirred for a further 5 h at room temperature. The solvent was removed under reduced pressure, and the resulting white crystalline product (yield 75−95%) was washed (3 × 15 mL) with diethyl ether. The phenylalanine methyl ester was coupled to Z-Ala-Ala in acetonitrile using 1 molar equiv of *O*-(benzotriazol-1-yl)-*N*,*N*,*N*′,*N*′-tetramethyluronium tetrafluoroborate and 0.2 molar equiv of 1-hydroxybenzotriazole as coupling reagents. After the mixture was stirred overnight at room temperature, the solvent was removed under reduced pressure and the crude product was dissolved in 200 mL of ethyl acetate. After being washed with 10% citric acid, saturated sodium carbonate, and sodium chloride, Z-Ala-Ala-Phe-OMe was purified by silica chromatography using either a dichloromethane/methanol or a petroleum ether/ethyl acetate mixture as an eluant. The peptidyl methyl ester was dissolved in dry methanol (10 cm^3/mol) containing 2 equiv of 2 M sodium hydroxide. The mixture was stirred at room temperature for 3−5 h until the reaction was complete. Solvent was removed under reduced pressure, and water was added to give a 0.5 M solution of product. After the product solution was cooled in an ice bath, the pH was slowly adjusted to 3−4 and the compound precipitated. It was filtered and dried to give the product as a white powder.

The typical yield was 0.47 g (1.05 mmol, 35%). ^{13}C NMR analysis gave the folowing data: δ_C (75.475 MHz, d_6-DMSO) 18.13 (1C, CH*C*H$_3$), 18.33 (1C, CH*C*H$_3$), 36.6 (1C, C$_6$H$_5$*C*H$_2$) 47.88 (1C, *C*HCH$_3$), 49.90 (1C, *C*HCH$_3$), 53.42 (1C, C$_6$H$_5$CH$_2$*C*H), 65.37 (1C, O*C*H$_2$Ph), 126.48−129.5 (10C, *C*H═*C*H), 137.03−137.37 (2C, CH═*C*═), 155.68 (1C, O*C*ONH), 172.11−172.69 (2C, *C*ONH, and 1C, *C*OOH).

Conversion of Z-Ala-Ala-Phe- and Z-Ala-Ala-[1-^{13}C]Phe into Z-Ala-Ala-Phe-glyoxal, Z-Ala-Ala-Phe-[1-^{13}C]glyoxal, and Z-Ala-Ala-Phe-[2-^{13}C]glyoxal. The amino-protected amino acid was dissolved in dry tetrahydrofuran (3 cm^3/mmol), the mixture was cooled to −30 °C, and 1.1 molar equiv of *N*-methylmorpholine was added. The mixture was warmed to −15 °C over 10 min and stirred at −15 °C for a further 15 min, and then 1 molar equiv of isobutyl chloroformate was added. The mixture was stirred for another 15 min at −15 °C, and then ∼4 molar equiv of freshly prepared diazomethane was added. The reaction was stirred for a further 4−5 h at −5 °C until complete. Solvent was removed under reduced pressure, and the product was purified by silica column chromatography using dichloromethane/methanol (98/2) as the eluant. This gave the product Z-Ala-Ala-Phe-diazoketone as an off white/yellow powder. The diazoketone was oxidized to the glyoxal using a procedure (*3*) modified from that of Ihmels (*19*). A 0.4 mmol portion of the diazoketone was oxidized to the glyoxal by dissolving it in a 5 mL solution of 0.1 M dimethyldioxirane in acetone and stirring until no more nitrogen was evolved. The reaction mixture was then moistened, and the acetone was removed by evaporation under reduced pressure. The moist compound was then dissolved in d_6-DMSO.

Scheme 1: Structures and Chemical Shifts of the Pepsin−Glyoxal Inhibitor Adducts

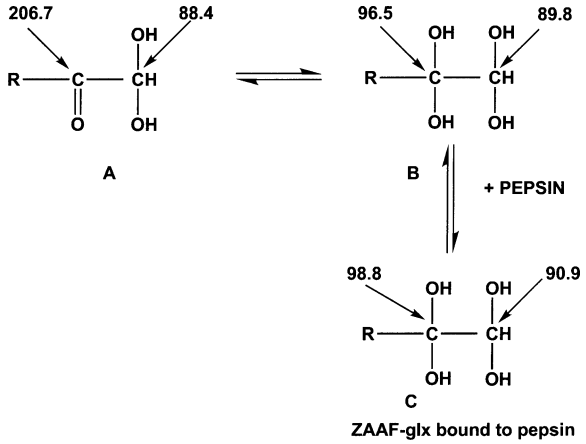

The typical yield was 0.32 g (0.72 mmol, 24%). ^{13}C NMR analysis gave the following data: δ_C (75.475 MHz, d_6-DMSO) 18.81 (2C, CH*C*H$_3$), 36.23 (1C, C$_6$H$_5$*C*H$_2$) 49.40 (1C, *C*HCH$_3$), 51.16 (1C, *C*HCH$_3$), 56.62 (1C, C$_6$H$_5$CH$_2$*C*H), 66.77 (1C, O*C*H$_2$Ph), 89.58 (1C, *C*OCH(OH)$_2$), 96.37 (1C, *C*(OH)$_2$CH(OH)$_2$), 127.56−130.21 (10C, *C*H═*C*H), 137.50 (1C, CH═*C*═), 138.11 (1C, CH═*C*═), 157.15 (1C, O*C*ONH), 173.77 (1C, *C*ONH), 174.10 (1C, *C*ONH), 206.44 (1C, *C*OCH(OH)$_2$).

The Z-Ala-Ala-Phe-[2-^{13}C]glyoxal was prepared using L-[1-^{13}C]phenylalanine, and in water the ^{13}C-enriched carbons gave characteristic signals at 206.7 and 96.5 ppm due to the glyoxal keto carbon and its hydrate, respectively (Scheme 1, structures A and B). *N*-[^{13}C]Methyl-*N*-nitrosotoluene-*p*-sulfonamide was used to generate the ^{13}C-enriched diazomethane used to synthesize Z-Ala-Ala-Phe-[1-^{13}C]glyoxal. In water there were two characteristic signals, one at 88.4 ppm and the other at 89.4 ppm (Scheme 1, structures A and B), for the ^{13}C-enriched hydrated glyoxal aldehyde carbon of Z-Ala-Ala-Phe-[1-^{13}C]glyoxal.

Enzyme Solutions. Salt-free crystallized pepsin from porcine gastric mucosa was obtained from Sigma Chemical Co. as a lyophilized powder with 3200−4500 units/mg of protein. One unit of activity produced $\partial A_{280} = 0.001$/min using hemoglobin as a substrate (*20*).

Inhibition of Pepsin by Glyoxal Inhibitors. Catalytic activity was measured using Phe-Ala-Ala-Phe(NO$_2$)Phe-Val-Leu-4-(hydroxymethyl)pyridine ester as a substrate (*21*). The substrate and inhibitor were dissolved separately in dimethyl sulfoxide. Samples for spectrophotometric analysis contained 3.3% (v/v) dimethyl sulfoxide and 0.1 M buffers at 25 °C. The amount of substrate present was determined using $\epsilon_{278} = 9472$ M^{-1} cm^{-1} (*21*). The total absorbance change

obtained from complete substrate hydrolysis was determined and used to calculate $\partial\epsilon_{310}$ at each pH studied. Mean $\partial\epsilon_{310}$ values of -150 and -310 M^{-1} cm^{-1} were obtained in 0.1 M oxalate buffer at pH 2 and 1, respectively. At pH 1 initial rates were obtained by following the first 10% of substrate hydrolysis. K_i values were estimated when $[S_o] \ll K_M$. Therefore, the equation for competitive inhibition ($d[P]/dt = (k_{cat}[E][S]/([S] + K_M(1 + [I]/K_i)$ reduces to $d[P]/dt = (k_{cat}/K_M)[E][S]/(1 + [I]/K_i)$. Therefore, a plot of $d[P]/dt$ versus [I] was subjected to a nonlinear regression analysis to determine K_i values. However, due to the lower molar extinction coefficients at pH 2, K_i values were estimated from complete progress curves obtained using substrate concentrations ~3 times the K_M value (*22*).

Determination of the Concentrations of Pepsin and Inhibitors. An M_r value of 34 600 (*23*) was used to estimate pepsin concentrations on the basis of weight, while protein concentrations were calculated using $\epsilon_{280} = 50\,900$ M^{-1} cm^{-1} (*24*). Concentrations of fully active pepsin were determined from the stoichiometry of inhibition with Z-Ala-Ala-Phe-[2-^{13}C]glyoxal (Figure 1A), and 65% of the pepsin protein was found to be fully active. Inhibitor concentrations were estimated using quantitative ^{13}C NMR spectroscopy (*25*). For Z-Ala-Ala-Phe-[2-^{13}C]glyoxal (~0.5 mM) the signals at 206.7 and 96.5 ppm had T_1 values of 2.2 ± 0.2 and 3.1 ± 0.2 s, and concentrations were estimated from integrated intensities of these proton-decoupled signals when they were fully relaxed using the integrated intensity of the signal at 171 ppm ($T_1 = 9.9 \pm 0.3$ s) from 20 mM oxalic acid buffer as a reference. The signals at 88.4 and 89.9 ppm from Z-Ala-Ala-Phe-[1-^{13}C]glyoxal had T_1 values of 0.32 ± 0.02 and 0.25 ± 0.01 s, respectively. Concentrations of Z-Ala-Ala-Phe-[1-^{13}C]glyoxal were determined the same way except that proton-coupled spectra were used for integrated intensity measurements.

NMR Spectroscopy. NMR spectra at 11.75 T were recorded with a Bruker Avance DRX 500 standard-bore spectrometer operating at 125.7716 MHz for ^{13}C nuclei. Sample tubes 10 mm in diameter were used. The spectral conditions for the samples of pepsin inhibited by Z-Ala-Ala-[2-^{13}C]Phe-glyoxal at 11.75 T were 32 768 time-domain data points, spectral width 241 ppm, acquisition time 0.54 s, 9.5 s relaxation delay time ($T_1 = 7.7 \pm 0.6$ s), 90° pulse angle, and 256 transients recorded per spectrum. Waltz-16 composite pulse ^{1}H decoupling with a BLARH100 amplifier was used with 16 dB attenuation during the acquisition time and 34 dB attenuation during the relaxation delay to minimize dielectric heating but maintain the nuclear Overhauser effect. The spectra were transformed using an exponential weighting factor of 10 Hz. Samples of pepsin inhibited by Z-Ala-Ala-[1-^{13}C]Phe-glyoxal were examined under the same conditions except that the acquisition time was 0.25 s, the relaxation delay was 1.1 s ($T_1 = 1.05 \pm 0.06$ s), and 1228−1536 transients were recorded per spectrum. The spectra were transformed using an exponential weighting factor of 20 Hz.

^{31}P NMR spectra at 11.75 T were recorded with a Bruker Avance DRX 500 standard-bore spectrometer operating at 202.45631 MHz for ^{31}P nuclei. Sample tubes 5 mm in diameter were used. The spectral conditions for the samples of pepsin inhibited by Z-Ala-Ala-[2-^{13}C]Phe-glyoxal at 11.75 T were 32 768 time-domain data points, spectral width 80 ppm, acquisition time 1.0 s, 9.7 s relaxation delay time, 90° pulse angle, and 174 transients recorded per spectrum. ^{1}H decoupling had a minimal effect on the line width and signal-to-noise ratio and so was not used. The spectra were transformed using an exponential weighting factor of 10 Hz.

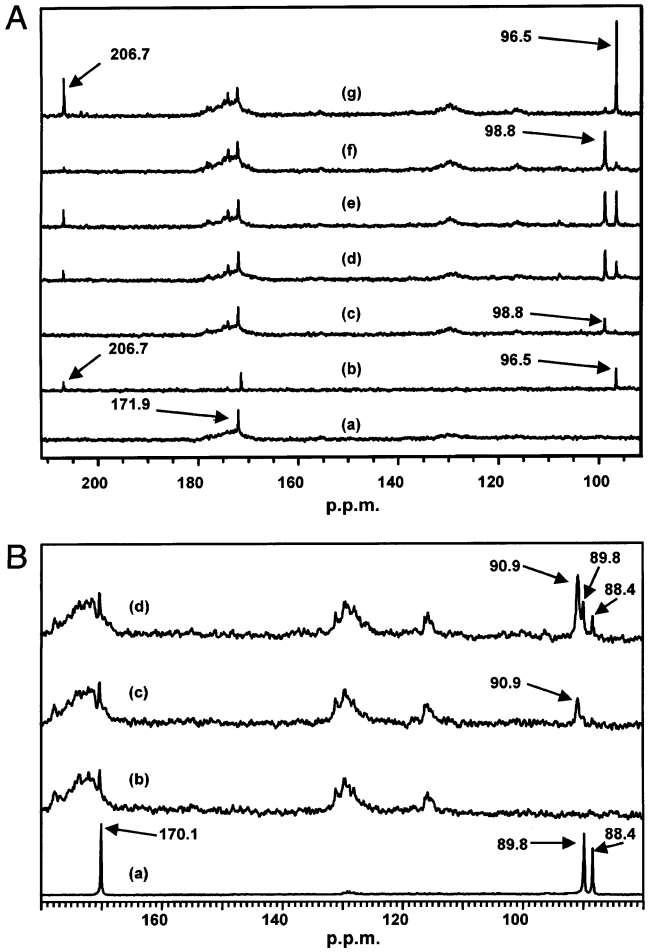

FIGURE 1: (A) ^{13}C NMR signals from Z-Ala-Ala-[2-^{13}C]Phe-glyoxal in the presence of pepsin. Acquisition and processing parameters were as described in the Materials and Methods. Sample conditions were (a) 2.90 mL of 0.59 mM pepsin at pH 4.32, (b) 2.98 mL of 0.25 mM Z-Ala-Ala-[2-^{13}C]Phe-glyoxal containing 0.34% (v/v) dimethyl sulfoxide at pH 4.30, (c) 2.93 mL of 0.59 mM pepsin and 0.77 mM Z-Ala-Ala-[2-^{13}C]Phe-glyoxal containing 0.52% (v/v) dimethyl sulfoxide at pH 4.31, (d) 2.95 mL of 0.58 mM pepsin and 1.15 mM Z-Ala-Ala-[2-^{13}C]Phe-glyoxal containing 1.53% (v/v) dimethyl sulfoxide at pH 4.33, (e) 2.95 mL of 0.58 mM pepsin and 1.27 mM Z-Ala-Ala-[2-^{13}C]Phe-glyoxal containing 1.7% (v/v) dimethyl sulfoxide at pH 4.36, (f) 2.95 mL of 0.92 mM pepsin and 1.27 mM Z-Ala-Ala-[2-^{13}C]Phe-glyoxal containing 1.7% (v/v) dimethyl sulfoxide at pH 4.37, and (g) 3.0 mL of 0.90 mM pepsin, 1.25 mM Z-Ala-Ala-[2-^{13}C]Phe-glyoxal, and 1.47 mM pepstatin containing 3.3% (v/v) dimethyl sulfoxide at pH 4.48. All samples contained 20 mM potassium oxalate to help stabilize the pH values and 10% (v/v) ^2H_2O to maintain a deuterium lock signal. (B) ^{13}C NMR signals from Z-Ala-Ala-[1-^{13}C]Phe-glyoxal in the presence of pepsin. Acquisition and processing parameters were as described in the Materials and Methods. Sample conditions were (a) 3.0 mL of 0.7 mM Z-Ala-Ala-[1-^{13}C]Phe-glyoxal in 0.1 M potassium formate containing 0.33% (v/v) dimethyl sulfoxide at pH 4.27, (b) 2.90 mL of 0.75 mM pepsin in 20 mM potassium formate containing 0.34% (v/v) dimethyl sulfoxide at pH 4.24, (c) 2.91 mL of 0.75 mM pepsin and 0.72 mM Z-Ala-Ala-[1-^{13}C]Phe-glyoxal in 20 mM potassium formate containing 0.34% (v/v) dimethyl sulfoxide at pH 4.24, and (d) 2.93 mL of 0.74 mM pepsin and 2.15 mM Z-Ala-Ala-[1-^{13}C]Phe-glyoxal in 20 mM potassium formate containing 1.53% (v/v) dimethyl sulfoxide at pH 4.25. All samples contained 10% (v/v) ^2H_2O to maintain a deuterium lock signal.

Both ^{1}H and ^{13}C chemical shifts are quoted relative to the peak for tetramethylsilane at 0.00 ppm. In aqueous solutions the chemical shift of the α-carbon of glycine was used as a chemical reference as described previously (*26*). ^{31}P chemical shifts were referenced to the peak for external 85% phosphoric acid at 0.00 ppm. For nonaqueous solvents, either 10% tetramethylsilane was used as an internal standard or an appropriate solvent signal was used as a secondary reference (*25*).

All aqueous samples contained 10% (v/v) $^{2}H_2O$ to obtain a deuterium lock signal, as well as 10 mM potassium phosphate buffer to help maintain stable pH values during pH titrations. For ^{31}P NMR spectra the potassium phosphate buffer was replaced by potassium formate buffer.

RESULTS

Inhibition of Pepsin Catalysis by Z-Ala-Ala-Phe-glyoxal. At pH 1.00 and 2.02 K_i values of 153 ± 1 and 89 ± 24 nM, respectively, were determined. This shows that this inhibitor is ~60 times more effective with pepsin at pH 2 than Z-Ala-Pro-Phe-glyoxal is at pH 7.0 with subtilisin (*6*) and is only ~3 times less effective than Z-Ala-Pro-Phe-glyoxal with δ-chymotrypsin at pH 7 (*3*).

^{13}C NMR Spectra of Pepsin Inhibited by Z-Ala-Ala-[2-^{13}C]Phe-glyoxal. Z-Ala-Ala-[2-^{13}C]Phe-glyoxal (Figure 1A, spectrum b) has signals at 206.7 and 96.5 ppm due to the inhibitor keto carbonyl carbon and its hydrate, respectively (Scheme 1, structures A and B). The signal at 171.9 ppm (Figure 1A, spectra a−g) is due to the oxalic acid buffer at pH 4.3. On addition of the inhibitor (Figure 1A, spectrum b) to pepsin in oxalic acid buffer (Figure 1A, spectrum a), the signals due to the free inhibitor at 96.5 and 206.7 ppm disappeared and a new signal at 98.8 ppm was observed (Figure 1A, spectrum c). On addition of an excess of inhibitor, the signals at 96.5 and 206.7 ppm due to the free inhibitor reappeared (Figure 1A, spectra d and e), but they were replaced by the signal at 98.8 ppm on addition of more pepsin (Figure 1A, spectrum f). Pepstatin is an extremely potent inhibitor of pepsin ($K_i \approx 1.1$ nM; *27*) and is therefore expected to displace the less tightly bound glyoxal inhibitor (Ki ~ 80 μM). Adding pepstatin led to the loss of the signal at 98.8 ppm and the reappearance of the signals at 96.5 and 206.7 ppm due to the unbound glyoxal inhibitor (Figure 1A, spectrum g). This confirmed that Z-Ala-Ala-[2-^{13}C]Phe-glyoxal is reversibly bound to pepsin (Scheme 1, structures C and B).

On the basis of measurements at 280 nm, it was estimated that 65.5% of the pepsin supplied was protein, and assuming inhibitor only bound to active enzyme, we estimate from our NMR results (Figure 1A) that 65% of the protein was fully active.

^{13}C NMR Spectra of Pepsin Inhibited by Z-Ala-Ala-[1-^{13}C]Phe-glyoxal. When Z-Ala-Ala-[1-^{13}C]Phe-glyoxal was added to pepsin (Figure 1B, spectrum b), the signals at 88.4 and 89.8 ppm (Figure 1B, spectrum a) due to the hydrated glyoxal aldehyde carbon (Scheme 1, structures A and B) were replaced by a single new signal at 90.9 ppm (Figure 1B, spectrum c). The signal at 170.1 ppm was due to the formic acid buffer used to maintain the pH at 4.2. On addition of an excess of the inhibitor, the signal at 90.9 ppm reached a maximal intensity and the signals due to the free inhibitor were observed at 88.4 and 89.8 ppm (Figure 1B, spectrum d). The signal at 90.9 ppm had a line width of 35.8−48.7 Hz at pH 0.97−6.82. Protonated carbons relax by dipolar relaxation and are expected to have line widths proportional to M_r (*28*, *29*). A methylene carbon rigidly attached to a protein with an M_r value of 35 000 would be expected to have a line width of 35−70 Hz (*30*, *31*). Therefore, the observed line widths for the new signal at 90.9 ppm observed in the presence of pepsin suggests that the inhibitor is rigidly bound to pepsin. Its chemical shift of 90.9 ppm is typical of an sp^3-hybridized carbon atom. This shows that it is the fully hydrated glyoxal that is bound by pepsin (Scheme 1, structure C).

Effect of pH on the ^{13}C NMR Signals from the Pepsin−Inhibitor Complexes Formed with Z-Ala-Ala-[1-^{13}C]Phe-glyoxal and Z-Ala-Ala-[2-^{13}C]Phe-glyoxal. The intensity of the signal at 90.9 ppm from the Z-Ala-Ala-[1-^{13}C]Phe-glyoxal bound to pepsin increased in as the pH decreased with a pK_a of 6.47 ± 0.15 (Figure 2a), and there was a concomitant decrease in the intensity of the signals due to the free inhibitor at 88.4 and 89.8 ppm (Figure 1 of the Supporting Information, spectra a−f). Below pH 4 there was no significant change in the ratio of the intensity of the signals at 88.4 and 89.4 ppm due to the free inhibitor and the signal at 90.9 ppm from the bound inhibitor (Figure 1 of the Supporting Information, spectra g−i). This demonstrates that the inhibitor is bound from pH 1 to pH 4 and that the inhibitor dissociation constant is <100 μM.

The intensity of the signal at 98.8 ppm from Z-Ala-Ala-[2-^{13}C]Phe-glyoxal bound to pepsin decreased as the pH increased according to a pK_a of 6.28 ± 0.08 (Figure 2b). As the intensity of the signal at 98.8 ppm due to the bound inhibitor decreased, there was a corresponding increase in the intensity of the signals at 96.5 and 206.7 ppm due to the free inhibitor (Figure 2 of the Supporting Information, spectra a−f). This demonstrates that the decrease in the intensity of the signal at 98.8 ppm is due to the pH-dependent disassociation of the inhibitor complex (Scheme 1, structures C and B). The pH-dependent changes in the inhibitor disassociation constant could be determined from these changes in signal intensity (Table 1), but spectrophotometric techniques had to be used to determine K_d values when the inhibitor was tightly bound.

When glyoxal inhibitors are incubated with the serine proteases chymotrypsin and subtilisin, there are pH-dependent changes in the chemical shift of the hemiketal carbon of the enriched carbon of the bound inhibitor which were used to show that the oxyanion pK_a was reduced to ~5 in chymotrypsin and <3 in subtilisin. However, with Z-Ala-Ala-[2-^{13}C]Phe-glyoxal bound to pepsin, no pH-dependent changes in the chemical shift of the bound signals at 98.8 ppm (Figure 2 of the Supporting Information) and 90.9 ppm (Figure 1 of the Supporting Information) were observed up to pH 6.8. Therefore, we conclude that the oxyanion pK_a must be >8 in the pepsin−Z-Ala-Ala-[2-^{13}C]-Phe-glyoxal complex.

Effect of pH on the Line Width of the ^{13}C NMR Signals from the Pepsin−Inhibitor Complexes Formed with Z-Ala-Ala-[1-^{13}C]Phe-glyoxal and Z-Ala-Ala-[2-^{13}C]Phe-glyoxal. The signal at 90.9 ppm due to the ^{13}C-enriched aldehyde carbon of the fully hydrated inhibitor bound to pepsin (Scheme 1, structure C) had a line width of 35.6 ± 3.8 Hz

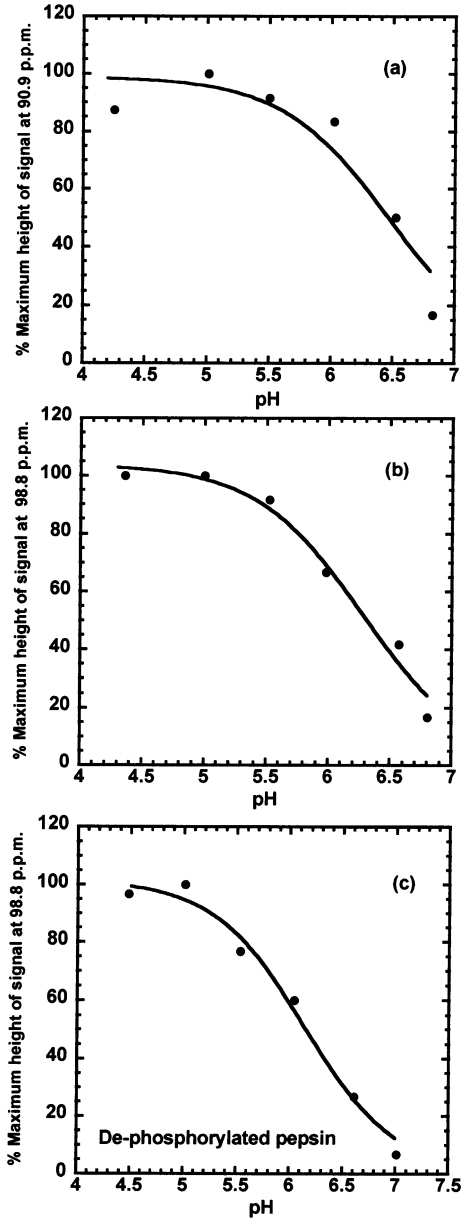

FIGURE 2: Effect of pH on the intensity of the ^{13}C NMR signals from Z-Ala-Ala-[1-^{13}C]Phe-glyoxal bound to pepsin and Z-Ala-Ala-[2-^{13}C]phe-glyoxal bound to pepsin and dephosphorylated pepsin. Experimental conditions are given in Figures 1 and 2 of the Supporting Information. Similar conditions were used for the studies with dephosphorylated pepsin. The continuous lines were calculated using the equation $I_{obsd} = I_{max}/(1 + K_{a1}/[H])$. The fitted parameters were (a) a signal at 90.9 ppm in the pepsin−Z-Ala-Ala-[1-^{13}C]Phe-glyoxal complex, pK_{a1} = 6.47 ± 0.15 and I_{max} = 99.0 ± 7.0%, (b) a signal at 98.7 ppm in the pepsin−Z-Ala-Ala-[2-^{13}C]Phe-glyoxal complex, pK_{a1} = 6.28 ± 0.08 and I_{max} = 103.9 ± 3.9%, and (c) a signal at 98.7 ppm in the dephosphorylated pepsin−Z-Ala-Ala-[2-^{13}C]Phe-glyoxal complex, pK_{a1} = 6.14 ± 0.08 and I_{max} = 101.6 ± 3.9%.

Table 1: Disassociation Constants for Z-Ala-Ala-Phe-glyoxal Bound to Pepsin at 25 °C

pH	K_i (μM)	method	pH	K_i (μM)	method
1.00	0.153	inhibition kinetics	5.98	487.0	NMR
2.02	0.089	inhibition kinetics	6.57	961.0	NMR
4.11	77.7	NMR	6.80	3512.0	NMR
5.52	225.0	NMR			

at pH 5.0−6.5 that increased to 48.7 ± 3.4 ppm at pH 0.97−4.25. The line width of the free inhibitor signal at 89.8 ppm (Scheme 1, structure B) increased from 12.5 ± 0.9 to 32.4 ± 0.9 ppm with decreasing pH according to a pK_a of 4.41 ± 0.1. However, the line width of the free inhibitor signal at 88.4 ppm (Scheme 1, structure A) had a much smaller line width which only increased by ~5 Hz from a value of 5.0 ± 0.6 Hz at pH 5.5−6.8 to a value of 10.3 ± 1.2 Hz. As separate signals are observed for the free and bound inhibitor, it is clear that they are not in fast exchange. The larger line broadening of ~20 Hz for the signal at 89.8 ppm is attributed to slow exchange broadening between the free (Scheme 1, structure B) and bound (Scheme 1, structure C) forms of the fully hydrated inhibitor. If the association rate constant (k_{on}) is diffusion controlled (~10^8 M^{-1} s^{-1}), then separate signals for the free and bound inhibitors will only be seen for tightly bound inhibitors with K_d values of less than ~1 μM (*32*). Separate signals are observed for both the free and bound inhibitor signals from pH 0.97 to pH 6.5 (Figure 1 of the Supporting Information). However, above pH 4 the K_d values are much larger than 1 μM (Table 1), showing that the association rate constant (k_{on}) must be significantly lower than the diffusion-controlled rate constant of ~10^8 M^{-1} s^{-1}. Similar slow association rates have been determined with the serine proteases subtilisin (*6*) and chymotrypsin (*2*). These slow association rates were attributed to the reaction of the active site serine hydroxyl with the ketone carbon of the glyoxal inhibitor to form a tetrahedral adduct analogous to the tetrahedral intermediate formed during catalysis by the serine proteases. Therefore, the binding of glyoxal inhibitors to the aspartyl proteases also involves a slow step, possibly a conformational change.

^{31}P NMR of Pepsin and of the Pepsin−Z-Ala-Ala-Phe-glyoxal Inhibitor Complex. When pepsin at pH 4.3 was examined by ^{31}P NMR, a signal at 0.91 ppm was observed (Figure 3a of the Supporting Information). The chemical shift of this signal is very similar to that (0.74 ppm) of inorganic phosphate at this pH (Figure 3b of the Supporting Information). Therefore, inorganic phosphate was added to pepsin to determine whether the signal at 0.91 ppm was due to inorganic phosphate. If it is due to inorganic phosphate, then only one signal would be observed if extra inorganic phosphate was added. On addition of inorganic phosphate to pepsin, it was found that two signals were observed, one at 0.91 ppm and the other at 0.74 ppm (Figure 3c of the Supporting Information). This confirms that the signal at 0.91 ppm is not due to inorganic phosphate. Dialysis of this sample against formate buffer at pH 4.3 did not affect this signal, but it did result in loss of the signal at 0.74 ppm due to inorganic phosphate. The signal at 0.74 ppm had a line width of 0.49 ± 0.07 Hz and a spin−lattice relaxation time of 8.25 ± 0.30 s typical of inorganic phosphate, while the signal at 0.91 ppm had a much broader line width of 24.6 ± 0.6 Hz and a shorter T_1 of 1.39 ± 0.13 s typical of a phosphorylated protein (*33*). These results confirm that the signal at 0.91 ppm is due to phosphate covalently attached to pepsin.

^{31}P NMR studies (*34*) on unfolded pepsinogen have shown that its phosphate group titrated with the same pK_a (5.82) as that of free phosphoserine, but as with other phosphoproteins the phosphate group of native pepsinogen titrated with a higher pK_a of 6.7 (Table 2). However, it was not known whether the pK_a of the phosphate group of pepsin was similar to that of the phosphate group of pepsinogen. In our work

Table 2: ^{31}P NMR pH Titration of Pepsin, Pepsinogen, Phosphoserine, and Inorganic Phosphate

compound	δ_1	δ_2	$\delta_1 - \delta_2$	pK_a	ref
inorganic phosphate	0.8	3.3	2.5	6.8	*33*
inorganic phosphate	0.79	3.28	2.49	6.94	present work
phosphoserine[a]	0.7−0.9	4.6−4.8	3.8−4.0	5.82	*33*
phosphoserine	0.70	4.54	3.84	5.81	present work
pepsinogen	∼1.5	∼5.0	∼3.5	6.70	*34*
pepsin	0.93	4.61	3.68	6.50	present work
pepsin and Z-Ala-Ala-Phe-glyoxal	0.88	4.63	3.75	6.44	present work

[a] Values (ppm) estimated from a graph.

Table 3: pK_a Values Determined from the pH-Dependent Changes in the Intensity of the ^{13}C NMR Signals from Z-Ala-Ala-[1-^{13}C]Phe-glyoxal Bound to Pepsin and Z-Ala-Ala-[2-^{13}C]Phe-glyoxal Bound to Pepsin and Dephosphorylated Pepsin

inhibitor	enzyme	signal monitored (ppm)	pK_a
Z-Ala-Ala-[1-^{13}C]Phe-glyoxal	pepsin	90.9	6.47
Z-Ala-Ala-[2-^{13}C]Phe-glyoxal	pepsin	98.7	6.28
Z-Ala-Ala-[2-^{13}C]Phe-glyoxal	dephosphorylated pepsin	98.7	6.14

(Figure 4 of the Supporting Information) the phosphate group of pepsin had titration parameters similar to those of pepsinogen (Table 2), but it had a slightly lower pK_a of 6.5, demonstrating that as in pepsinogen the pK_a of the phosphoserine phosphate group of pepsin is raised relative to the value in free phosphoserine (Table 2). Binding Z-Ala-Ala-[2-^{13}C]Phe-glyoxal did not significantly change the pK_a of the pepsin phosphate group (Table 2). This pK_a is very similar to those obtained from pH-dependent changes in the intensity of ^{13}C NMR signals at 90.9 ppm (Figure 2a) and 98.7 ppm (Figure 2b) obtained from studies on the Z-Ala-Ala-[1-^{13}C]Phe-glyoxal− and Z-Ala-Ala-[2-^{13}C]Phe-glyoxal− pepsin complexes, respectively (Table 3). However, when dephosphorylated pepsin was bound to Z-Ala-Ala-[2-^{13}C]-Phe-glyoxal, there was only a small decrease in the pK_a (Table 3) obtained from the pH-dependent changes in the intensity of the signal at 98.7 ppm (Figure 2c). This shows that the pK_a values (Table 3) determined from the pH-dependent changes in the intensities of the ^{13}C NMR signals at 90.9 and 98.7 ppm are not significantly affected by the phosphate group of pepsin. Since the pH-dependent changes in the intensities of these signals reflect the amount of bound inhibitor, then these results show that the phosphate group of pepsin does not have a significant role in binding inhibitors.

^{1}H NMR of the Hydrogen-Bonded Protons of Pepsin, a Pepsin−Pepstatin Inhibitor Complex, and the Pepsin−Z-Ala-Ala-Phe-glyoxal Inhibitor Complex. Hydrogen-bonded protons have chemical shifts in the range 11−22 ppm, with the stronger hydrogen bonds having more deshielded protons at higher chemical shifts. Particularly strongly hydrogen-bonded protons with chemical shifts in the range 16−20 ppm are classified as low-barrier hydrogen bonds (*35*).

With pepsin four proton signals were detected which had chemical shifts >11.0 ppm (Figure 3A). These were at ∼11.2, ∼12.0, 13.2, and 13.6 ppm (Figure 3A, spectrum 3). The signal at ∼12 ppm had a small titration shift from 12.03 ± 0.01 to 11.83 ± 0.01 ppm with increasing pH according to a pK_a of 3.22 ± 0.19 (Figure 4A). The pH dependence of k_{cat}/K_M for neutral substrates gives a bell-shaped pH dependence with rates increasing with a pK_1 of 1.1−1.4 and decreasing with a pK_2 of 3.5−4.8 (*36*, *37*). It is therefore possible that the pH-dependent decrease in the chemical shift of the signal at ∼12.0 ppm is due to the catalytic group causing the decrease in k_{cat}/K_M. However, pepsin has a large number of acidic residues, any one of which could be causing this decrease in chemical shift. When pepsin was incubated with a 50% molar excess of Z-Ala-Ala-Phe-glyoxal at 25 °C, a similar titration shift from 12.08 ± 0.01 to 11.92 ± 0.01 with a pK_a of 3.38 ± 0.19 was observed (Figure 4B). This pK_a was essentially the same as that observed with free pepsin. In the presence of a 50% molar excess of pepstatin a similar titration shift from 12.04 ± 0.01 to 11.88 ± 0.01 ppm was observed (Figure 4C) except that the pK_a was lowered to 2.69 ± 0.08. Similar decreases of 0.2−0.65 in pK_2 values have been estimated from pH-dependent changes in k_{cat} (*37*). The K_i values (Table 1) confirm that the inhibitor was bound to pepsin from pH 1 to pH 5, demonstrating that the binding of Z-Ala-Ala-Phe-glyoxal to pepsin does not significantly perturb this enzyme pK_a but pepstatin binding lowers it by ∼0.7 pK_a unit.

The chemical shift of the other three signals in pepsin did not change with pH. However, the intensity of the signal at 13.6 ppm showed a bell-shaped dependence on pH (Figure 5A). Similar results were obtained for the signals at 13.2, 12.0, and 11.1 ppm (Table 4). The pK_1 for the ascending limb of the bell was ∼1.2 (Table 4) and is essentially the same as the pK_1 values obtained from the pH dependence of k_{cat}/K_M. For pepsin two of the pK_2 values obtained from the descending limb of the bell are ∼5 (Table 4) and similar to the pK_2 values of 3.5−4.8 obtained from the pH dependence of k_{cat}/K_M. However, the other two pK_2 values of 6.95 and 7.29 (Table 4) are significantly larger than the corresponding pK_2 values of 3.5−4.8 determined from the pH dependence of k_{cat}/K_M. The intensity of the signal at 13.6 ppm also showed a bell-shaped pH dependence in the presence of Z-Ala-Ala-Phe-glyoxal (Figure 5B) and pepstatin (Figure 5C). Similar results were obtained for the signals at 13.2, 12.0, and 11.1 ppm (Table 4).

The Z-Ala-Ala-Phe-glyoxal−pepsin inhibitor complex was examined at 25 °C, and it was found that as with free pepsin four signals were detected which had chemical shifts >11.0 ppm (Figure 3B). These were at ∼11.1, ∼12.1, 13.3, and 13.6 ppm (Figure 3B, spectrum 4). Therefore, we can conclude that none of the four hydroxyl groups (Scheme 1, structure C) of the bound hydrated glyoxal are involved in strong hydrogen bonds with pepsin.

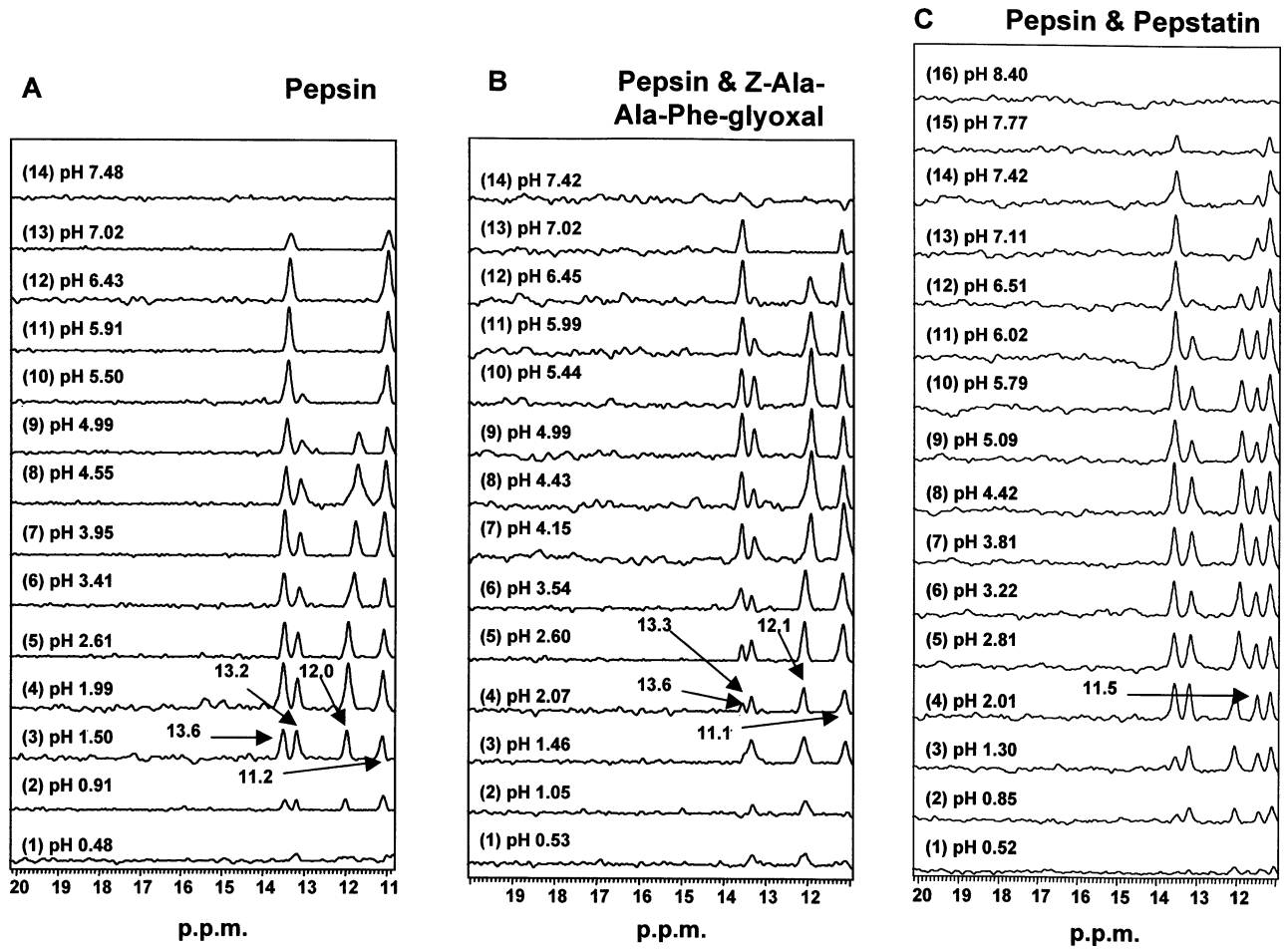

FIGURE 3: pH dependence of the ^{1}H NMR spectra of pepsin and of its complexes with Z-Ala-Ala-Phe-glyoxal and pepstatin at 25 °C. Acquisition and processing parameters were as described in the Materials and Methods. All samples were 0.5 mL, and they were made with fresh samples of pepsin and if indicated fresh samples of inhibitor in a 10 mM buffer. The buffers used were sodium formate (pH 0.3−5.0), sodium phosphate (pH 5.75−7.0), and Tris−HCl (pH 7.4−8.4). (A) Pepsin. Sample conditions were 0.113 mM pepsin. (B) Pepsin and Z-Ala-Ala-Phe-glyoxal. Sample conditions were 0.74 mM pepsin, 1.02 mM Z-Ala-Ala-[1-^{13}C]Phe-glyoxal, and 0.23% (v/v) dimethyl sulfoxide. (C) Pepsin and pepstatin. Sample conditions were 0.109 mM pepsin, 0.149 mM pepstatin, and 0.5% (v/v) dimethyl sulfoxide. All samples were at 25 °C, and they contained 10% (v/v) ^2H_2O to maintain a deuterium lock signal.

In the presence of a 50% excess of pepstatin the pK_1 values are not significantly perturbed (Table 4). However, the values of pK_2 (Table 4) are significantly raised by 0.5−1.4 pK_a units relative to their values in free pepsin. In the presence of pepstatin, signals at 13.5, 13.2, 12.0, and 11.2 ppm were observed (Figure 3C, spectrum 4) and a new signal at 11.5 ppm was also detected (Figure 3C, spectra 2−14).

These pH-dependent changes in signal height were not accompanied by significant changes in chemical shift, so they represent a slow exchange process. The increases in pK_a values observed on binding pepstatin could be explained if the ionizing groups were neutral acids and if pepstatin binding caused a decrease in the effective dielectric constant for these groups. Pepstatin binding could decrease the dielectric constant either by causing a conformational change in pepsin and/or by directly shielding these groups from the aqueous solvent.

Studies at 3, 10, 25, and 37 °C showed that the intensities of the signals above 11.0 ppm were maximal at 25 °C but only decreased slightly at the other temperatures (data not shown).

With free pepsin and the pepsin−pepstatin complex pK_1 was 1.2 ± 0.3 for all the signals except for the signal at 13.6 ppm in the pepsin−pepstatin complex where pK_1 was 1.61 ± 0.16. This pK_a is even larger at 2.94 ± 0.15 in the pepsin−Z-Ala-Ala-Phe-glyoxal complex (Table 4). The pK_2 values observed for the pepsin−Z-Ala-Ala-Phe-glyoxal complex are similar to those observed in free pepsin and in the pepsin−pepstatin complex (Table 4).

DISCUSSION

The pH dependence of k_{cat} for the pepsin-catalyzed hydrolysis of Ac-Phe-Tyr-OMe is bell shaped, and dephosphoryalation of pepsin led to a 10% decrease in the limiting value for k_{cat} and an increase of 0.5 pK_a unit in both pK_a values (*38*). These small changes led the authors to conclude that the phosphate group in pepsin is not involved in the catalytic mechanism (*38*). Our results showing that dephosphorylation does not significantly affect the pH dependence of the binding of glyoxal inhibitors (Table 3) supports this conclusion. Further support for this conclusion comes from the fact that the phosphorus atom of phosphoserine-68 is ~30 Å from the carbons of the active site carboxylate groups of aspartate-32 and -215 (*39*).

Our failure to detect oxyanion formation provides no evidence for oxyanion stabilization by pepsin and is con-

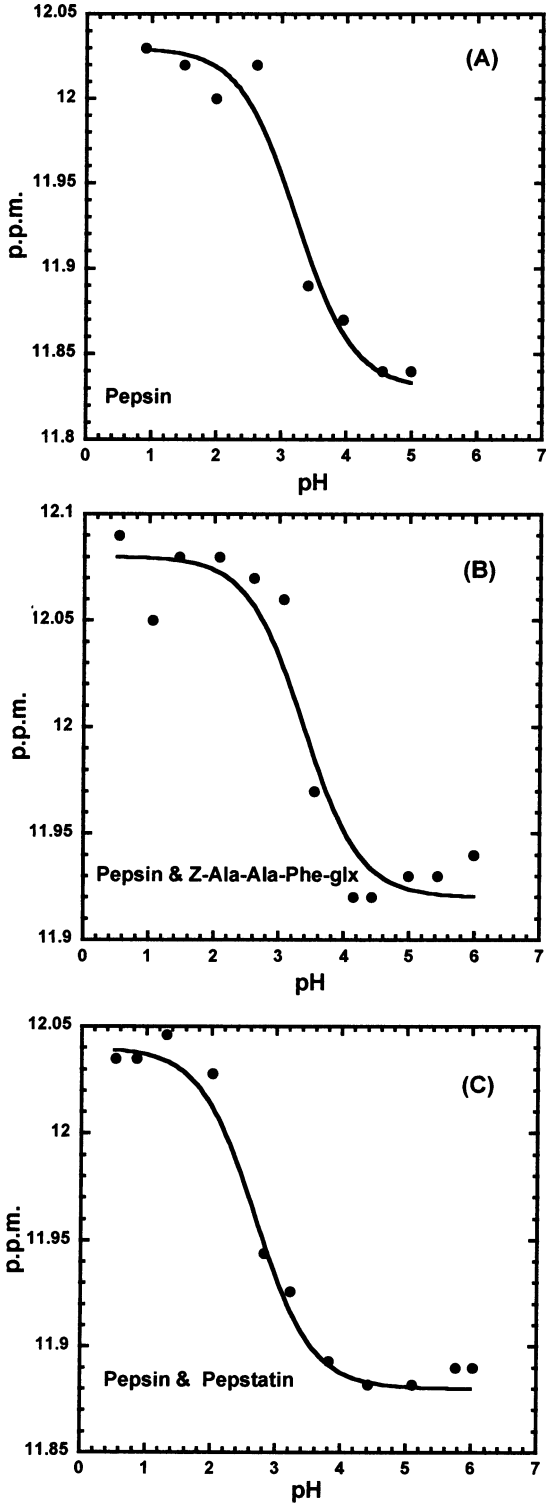

FIGURE 4: pH dependence of the signal at ~12 ppm in the ^{1}H NMR spectra of pepsin and of its complexes with Z-Ala-Ala-Phe-glyoxal and pepstatin at 25 °C. Acquisition parameters were as described in the Materials and Methods. Sample conditions were as described in the caption to Figure 3. The continuous lines were calculated using the following equation: $\delta_{obsd} = S_1/(1 + K_a/[H]) + S_2/(1 + [H]/K_a)$. **(**A**)** Pepsin. The continuous line was calculated using the fitted parameters p$K_a = 3.22 \pm 0.19$, $S_1 = 11.83 \pm 0.01$ ppm, and $S_2 = 12.03 \pm 0.01$ ppm. **(**B**)** Pepsin and Z-Ala-Ala-Phe-glyoxal. The continuous line was calculated using the fitted parameters p$K_a = 3.38 \pm 0.19$, $S_1 = 12.08 \pm 0.01$ ppm, and $S_2 = 11.92 \pm 0.01$ ppm. **(**C**)** Pepsin and pepstatin. The continuous line was calculated using the fitted parameters p$K_a = 2.69 \pm 0.08$, $S_1 = 11.88 \pm 0.01$ ppm, and $S_2 = 12.04 \pm 0.01$ ppm.

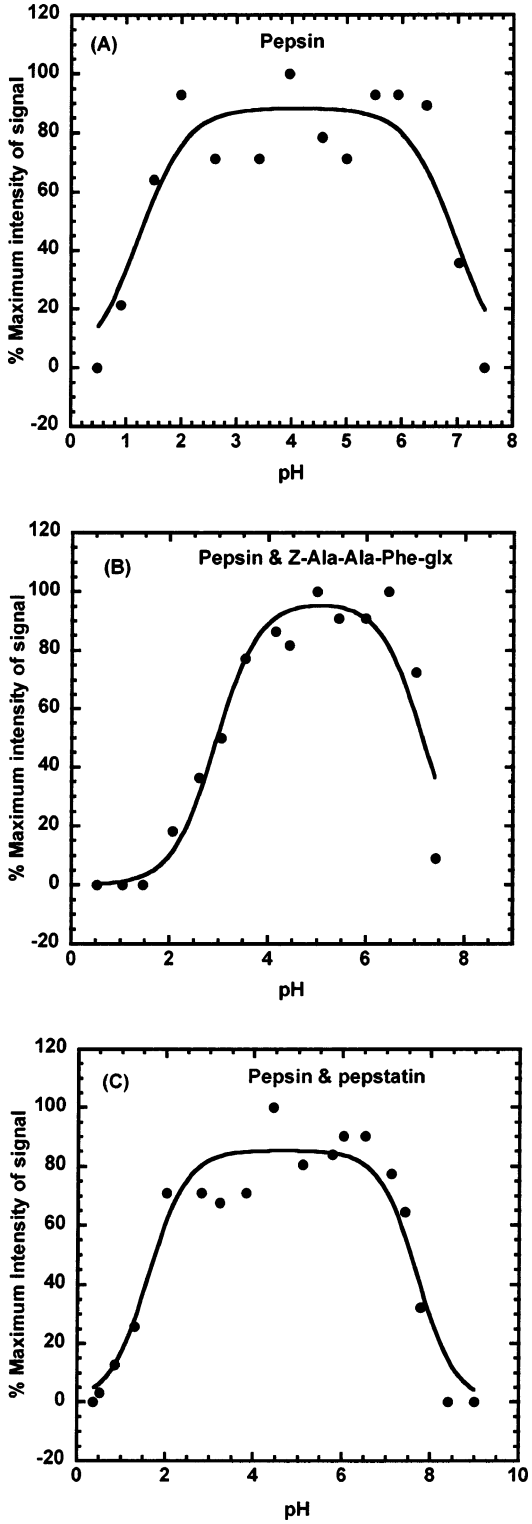

FIGURE 5: Effect of pH on the intensity of the ^{1}H NMR signals at ~13.6 ppm from pepsin and from pepsin bound to Z-Ala-Ala-[2-^{13}C]Phe-glyoxal and to pepstatin. Acquisition parameters were as described in the Materials and Methods. Sample conditions were as described in the caption to Figure 3. The continuous lines were calculated using the following equation: $I_{obsd} = I_{max}/(1 + [H]/K_a + K_a/[H])$. **(**A**)** Pepsin. The continuous line was calculated using the fitted parameters p$K_1 = 1.23 \pm 0.22$, p$K_2 = 6.95 \pm 0.23$, and $I_{max} = 88.5 \pm 6.1\%$. **(**B**)** Pepsin and Z-Ala-Ala-Phe-glyoxal. The continuous line was calculated using the fitted parameters p$K_1 = 2.94 \pm 0.15$, p$K_2 = 7.18 \pm 0.16$, and $I_{max} = 96.7 \pm 5.6\%$. **(**C**)** Pepsin and pepstatin. The continuous line was calculated using the fitted parameters p$K_1 = 1.61 \pm 0.16$, p$K_2 = 7.71 \pm 0.14$, and $I_{max} = 85.4 \pm 3.7\%$.

Table 4: pK_a Values Determined at 25 °C from pH-Dependent Changes in the Intensities of the NMR Signals from 11.1 to 13.6 ppm

compound	monitored species, signal (ppm)	pK_1	pK_2
pepsin	Ht, 13.6	1.23 ± 0.22	6.95 ± 0.23
pepsin	Ht, 13.2	0.83 ± 0.29	5.17 ± 0.30
pepsin	Ht, 12.0	1.20 ± 0.28	4.94 ± 0.26
pepsin	Ht, 11.1	1.26 ± 0.27	7.29 ± 0.40
pepsin−ZAAFglx	Ht, 13.6	2.94 ± 0.15	7.18 ± 0.16
pepsin−ZAAFglx	Ht, 13.2	0.90 ± 0.29	6.32 ± 0.28
pepsin−ZAAFglx	Ht, 12.0	1.78 ± 0.22	6.46 ± 0.21
pepsin−ZAAFglx	Ht, 11.1	1.86 ± 0.19	6.93 ± 0.18
pepsin−pepstatin	Ht, 13.6	1.61 ± 0.16	7.71 ± 0.14
pepsin−pepstatin	Ht, 13.2	1.02 ± 0.16	6.16 ± 0.17
pepsin−pepstatin	Ht, 12.0	1.13 ± 0.12	6.30 ± 0.12
pepsin−pepstatin	Ht, 11.5	1.15 ± 0.15	7.24 ± 0.15
pepsin−pepstatin	Ht, 11.1	1.17 ± 0.16	7.82 ± 0.17

sistent with catalysis proceeding via a concerted mechanism involving a neutral tetrahedral intermediate. Neutral phosphinic acid inhibitors of the HIV-1 protease are bound more tightly than their negatively charged forms (*40*), confirming that the aspartyl proteases preferentially bind neutral tetrahedral intermediates.

It has been suggested that there may be short strong hydrogen bonds in HIV-1 protease complexes (*15*), and ab initio calculations have led to the suggestion that there is a low-barrier hydrogen bond between the catalytic carboxylate groups of HIV protease (*41*). It has also been argued that the pK_a shifts due to deuterium oxide show the presence of low-barrier hydrogen bonds in free pepsin (*42*), but these data have been criticized (*43*). Our ^{1}H NMR studies on pepsin (Figure 3) and earlier ^{1}H NMR studies on β-secretase (*16*) and endothiapepsin (*44*) have not detected any low-barrier hydrogen bonds in free aspartyl proteases. Therefore, we conclude that there is not a low-barrier hydrogen bond between the catalytic carboxylate groups of the aspartyl proteases in the absence of ligands.

From X-ray studies of a HIV protease product complex it has been reported that the inner oxygen atoms of the catalytic aspartate residues are only 2.3 Å apart, which has led to the conclusion that a low-barrier hydrogen bond is formed in this crystalline product complex (*45*). A short hydrogen bond has also been predicted by quantum-classical molecular dynamics simulations (*46*). Short strong (low-barrier) hydrogen bonds are said to be formed when the O···O distance is 2.5 Å or less. A distance of 2.29 Å is the limit, and a distance of 2.3 Å should result in a single well hydrogen bond which would be extremely strong (*47*−*49*). This would imply either that a transition-state analogue has been formed or that the enzyme structure has been abnormally perturbed in the crystalline product complex. Hydrogen bonds can be very strong in crystals, so such strong hydrogen bonds may not be observable in solution. For optimal catalytic efficiency products should not be tightly bound, so it is unlikely that a strong hydrogen bond would be detected in a product complex in solution.

The fact that pepsin preferentially binds the fully hydrated form of the glyoxal inhibitor suggests that pepsin utilizes transition-state stabilization and not ground-state stabilization to achieve catalytic efficiency. This conclusion is supported by the fact that fluoroketone inhibitors ($RCOCF_2R'$) are ∼10 times more effective than their alcohol analogues ($RCHOHCH_2R'$) (*50*, *51*). This increased inhibitor effectiveness has been attributed to the fact that the fluoroketone is hydrated ($RC(OH)_2CH_2R'$) and closely resembles the catalytic transition state (*51*). The better binding presumably results from hydrogen bonding to both hydroxyl groups. With glyoxal inhibitors, binding could involve all four hydroxyl groups and tight binding could also be facilitated if these hydroxyl groups formed low-barrier hydrogen bonds with pepsin. However, our results show that low-barrier hydrogen bonds are not involved in the binding of glyoxal inhibitors, and we are unable to detect any new hydrogen bonds being formed on glyoxal inhibitor binding.

^{1}H NMR experiments with β-secretase at 20 °C and pH 4.5 have shown only one signal at 11.8 ppm in the absence of inhibitors (*16*). However, as in our work with pepstatin (Figure 3C) an additional signal was observed on addition of a 50% excess of OM99-2, a potent hydroxymethylene inhibitor of β-secretase. The new signal was at 13.0 ppm, but there was no evidence of the signals at 11.2, 11.5, 12.0, 13.2, and 13.5 ppm observed in the present work with pepsin (Figure 3C). In contrast studies on endothiapepsin at 10 °C and pH 4.5 did not detect any signals at pH > 11.0 with the free enzyme (*17*, *18*). However, on addition of statine or *gem*-diol inhibitors two new signals were detected, one at ∼12.0 ppm and the other at 16.1 ppm, which was assigned to a hydrogen bond involving the statine hydroxyl group (*17*, *18*). The new signal that appeared on addition of pepstatin to pepsin was at a much lower chemical shift of 11.5 ppm (Figure 3C, spectra 2−14). Therefore, if we assign this signal to the pepstatin hydroxymethylene proton, then it is clear that the proton of the pepstatin hydroxyl group is not involved in a strong hydrogen bond in the pepsin−pepstatin inhibitor complex. The absence of a ^{1}H NMR signal with a chemical shift >15 ppm confirms that a strong hydrogen bond/low-barrier hydrogen bond is not formed in the pepsin−pepstatin inhibitor complex.

Hydrogen bonds involving charged groups are stronger than those involving neutral groups (*52*), so it is not surprising that a strong hydrogen bond is formed between the positively charged active site histidine (histidine-57) and the negatively charged active site aspartate-102 residue in both free α-chymotrypsin (*53*−*55*) and α-chymotrypsin−glyoxal inhibitor complexes (*2*). The absence of a strong hydrogen bond in the pepsin−pepstatin inhibitor reflects the fact that pepsin catalysis proceeds via a concerted mechanism involving a neutral tetrahedral intermediate, so it stabilizes neutral tetrahedral adducts which form neutral hydrogen bonds that are weaker than hydrogen bonds involving charged groups.

The preferential binding of hydrated carbonyl groups suggests that the aspartyl proteases must stabilize these hydrates by hydrogen bonding. As these hydrogen bonds are not low-barrier/strong hydrogen bonds, the primary role of these hydrogen bonds in catalysis must be to optimally orientate the hydrated peptide carbonyl of the peptide bond being hydrolyzed.

SUPPORTING INFORMATION AVAILABLE

Figure 1, ^{13}C NMR spectra showing the effect of pH on the intensity of the ^{13}C NMR signals from Z-Ala-Ala-[1-^{13}C]Phe-glyoxal bound to pepsin, Figure 2, effect of pH on

the intensity of the ^{13}C NMR signals from Z-Ala-Ala-[2-^{13}C]Phe-glyoxal bound to pepsin, Figure 3, ^{31}P NMR of pepsin and free phosphate, and Figure 4, effect of pH on the chemical shifts of the phosphorus atoms in phosphoserine and pepsin. This material is available free of charge via the Internet at http://pubs.acs.org.

REFERENCES

1. Darkins, P., McCarthy, N., McKervey, M. A., and Ye, T. (1993) Oxidation of alpha-Diazoketones derived from L-Amino Acids and Dipeptides using Dimethyldioxirane. Synthesis and Reactions of Homochiral N-Protected α-Amino Glyoxals, *J. Chem. Soc., Chem. Commun. 15*, 1222−1223.
2. Spink, E., Cosgrove, S., Rogers, L., Hewage, C., and Malthouse, J. P. (2007) ^{13}C- and ^{1}H-NMR studies of ionisations and hydrogen bonding in chymotrypsin-glyoxal inhibitor complexes, *J. Biol. Chem. 282*, 7852−7861.
3. Djurdjevic-Pahl, A., Hewage, C., and Malthouse, J. P. G. (2002) A ^{13}C-NMR study of the inhibition of d-chymotrypsin by a tripeptide-glyoxal inhibitor, *Biochem. J. 362*, 339−347.
4. Murphy, E. A., O'Connell, T. P., and Malthouse, J. P. G. (1996) The synthesis and characterisation of a glyoxal inhibitor of chymotrypsin, *Biochem. Soc. Trans. 24*, 129S.
5. Walker, B., McCarthy, N., Healy, A., Ye, T., and McKervey, M. A. (1993) Peptide glyoxals: a novel class of inhibitor for serine and cysteine proteinases, *Biochem. J. 293*, 321−323.
6. Djurdjevic-Pahl, A., Hewage, C., and Malthouse, J. P. G. (2005) Ionisations within a subtilisin-glyoxal inhibitor complex, *Biochim. Biophys. Acta 1749*, 33−41.
7. Lowther, J., Djurdjevic-Pahl, A., Hewage, C., and Malthouse, J. P. G. (2002) A ^{13}C-NMR study of the inhibition of papain by a dipeptide-glyoxal inhibitor, *Biochem. J. 366*, 983−987.
8. Lynas, J. F., Hawthorne, S. J., and Walker, B. (2000) Development of Peptidyl α-keto-*β*-aldehydes as New Inhibitors of Cathepsin L-Comparisons of Potency and Selectivity Profiles with Cathepsin B, *Bioorg. Med. Chem. Lett. 10*, 1771−1773.
9. Walker, B., Lynas, J. F., Meighan, M. A., and Bromme, D. (2000) Evaluation of Dipeptide α-Keto-*β*-aldehydes as New Inhibitors of Cathepsin S, *Biochem. Biophys. Res. Commun. 275*, 401−405.
10. Lynas, J. F., Harriott, P., Healy, A., McKervey, M. A., and Walker, B. (1998) Inhibitors of the chymotrypsin-like activity of proteasome based on di- and tri-peptidyl α-keto aldehydes (glyoxals), *Bioorg. Med. Chem. Lett. 8*, 373−378.
11. Qasmi, D., de Rosny, E., Rene, L., Badet, B., Vergely, I., Boggetto, N., and Reboud-Ravaux, M. (1997) Synthesis of N-glyoxylyl peptides and their in vitro evaluation as HIV-1 protease inhibitors, *Bioorg. Med. Chem. 5*, 707−714.
12. Pauling, L. (1946) Molecular architecture and biological reactions, *Chem. Eng. News 24*, 1375−1377.
13. Wolfenden, R. (1976) Transition state analog inhibitors and enzyme catalysis, *Annu. Rev. Biophys. Bioeng. 5*, 271−306.
14. Davies, D. R. (1990) The structure and function of the aspartic proteinases, *Annu. Rev. Biophys. Biophys. Chem. 19*, 189−215.
15. Meek, T. D. (1998) Catalytic mechanisms of the aspartic proteinases, *Comprehensive Biological Catalysis*, pp 327−344, Academic Press, New York.
16. Toulokhonova, L., Metzler, W. J., Witmer, M. R., Copeland, R. A., and Marcinkeviciene, J. (2003) Kinetic studies on beta-site amyloid precursor protein-cleaving enzyme (BACE). Confirmation of an iso mechanism, *J. Biol. Chem. 278*, 4582−4589.
17. Coates, L., Erskine, P. T., Crump, M. P., Wood, S. P., and Cooper, J. B. (2002) Five atomic resolution structures of endothiapepsin inhibitor complexes: implications for the aspartic proteinase mechanism, *J. Mol. Biol. 318*, 1405−1415.
18. Coates, L., Erskine, P. T., Mall, S., Gill, R., Wood, S. P., Myles, D. A., and Cooper, J. B. (2006) X-ray, neutron and NMR studies of the catalytic mechanism of aspartic proteinases, *Eur. Biophys. J. 35*, 559−566.
19. Ihmels, H., Maggini, M., Prato, M., and Scorrano, G. (1991) Oxidation of Diazo Compounds by Dimethyl Dioxirane:an Extremely Mild and Efficient Method for the Preparation of Labile α-Oxo-Aldehydes, *Tetrahedron Lett. 32*, 6215−6218.
20. Anson, M. L., and Mirsky, A. E. (1932) The Estimation of pepsin with Hemoglobin, *J. Gen. Physiol. 16*, 59−63.
21. Agarwal, N., and Rich, D. H. (1983) An improved cathepsin-D substrate and assay procedure, *Anal. Biochem. 130*, 158−165.
22. Waley, S. G. (1982) A quick method for the determination of inhibition constants, *Biochem. J. 205*, 631−633.
23. Green, B. N., Jones, A. T., and Roberts, N. B. (1996) Electrospray mass spectrometric evidence for the occurrence of two major variants in native pig pepsin A, *Biochem. J. 313* (Pt 1), 241−244.
24. Hollands, T. R., Voynick, I. M., and Fruton, J. S. (1969) Action of pepsin on cationic synthetic substrates, *Biochemistry 8*, 575−585.
25. Wehrli, F. W., Marchand, A. P., and Wehrli, S. (1988) Interpretation of Carbon-13 NMR Spectra, *Interpretation of Carbon-13 NMR Spectra*, p 34, John Wiley & Sons, Chichester, U.K.
26. Finucane, M. D., Hudson, E. A., and Malthouse, J. P. G. (1989) A ^{13}C-n.m.r. investigation of the ionizations within an inhibitor-alpha-chymotrypsin complex: Evidence that both alpha-chymotrypsin and trypsin stabilize a hemiketal oxyanion by similar mechanisms, *Biochem. J. 258*, 853−859.
27. Marciniszyn, J., Jr., Hartsuck, J. A., and Tang, J. (1976) Mode of inhibition of acid proteases by pepstatin, *J. Biol. Chem. 251*, 7088−7094.
28. Doddrell, D., Glushko, V., and Allerhand, A. (1972) Theory of Nuclear Overhauser Enhancement and ^{13}C-^{1}H dipolar Relaxation in Proton-Decoupled Carbon-13 NMR Spectra of Macromolecules, *J. Chem. Phys. 56*, 3683−3689.
29. Oldfield, E., Norton, R. S., and Allerhand, A. (1975) Studies of Individual Carbon Sites of proteins in Solution by Natural Abundance Carbon 13 Nuclear Magnetic resonance Spectroscopy, *J. Biol. Chem. 250*, 6368−6380.
30. Malthouse, J. P. G. (1986) ^{13}C NMR of Enzymes, *Prog. Nucl. Magn. Reson. Spectrosc. 18*, 1−60.
31. Malthouse, J. P. G., and Finucane, M. D. (1991) A study of the relaxation parameters of a ^{13}C-enriched methylene carbon and a ^{13}C-enriched perdeuteromethylene carbon attached to chymotrypsin, *Biochem. J. 280*, 649−657.
32. Feeney, J., Batchelor, J. G., Albrand, J. P., and Roberts, G. C. K. (1979) The Effects of Intermediate Exchange Processes on the Estimation of Equilibrium Constants by NMR, *J. Magn. Reson. 35*, 519−529.
33. Brauer, M., and Sykes, B. D. (1984) Phosphorus-31 nuclear magnetic resonance studies of phosphorylated proteins, *Methods Enzymol. 107*, 36−81.
34. Williams, S. P., Bridger, W. A., and James, M. N. (1986) Characterization of the phosphoserine of pepsinogen using ^{31}P nuclear magnetic resonance: corroboration of X-ray crystallographic results, *Biochemistry 25*, 6655−6659.
35. Frey, P. A., Whitt, S. A., and Tobin, J. B. (1994) A Low-Barrier Hydrogen Bond in the Catalytic Triad of Serine Proteases, *Science 264*, 1927−1930.
36. Cornish-Bowden, A. J., and Knowles, J. R. (1969) The pH Dependence of Pepsin-Catalysed Reactions, *Biochem. J. 113*, 353−362.
37. Denburg, J. L., Nelson, R., and Silver, M. S. (1968) The Effect of pH on the Rates of Hydrolysis of Three Acylated Dipeptides by Pepsin, *J. Am. Chem. Soc. 90*, 479−486.
38. Clement, G. E., Rooney, J., Zakheim, D., and Eastman, J. (1970) The pH Dependence of the Dephosphorylated Pepsin-Catalysed Hydrolysis of N-Acetyl-L-Phenylalanyl-L-tyrosine Methyl Ester, *J. Am. Chem. Soc. 92*, 186−189.
39. Sielecki, A. R., Fedorov, A. A., Boodhoo, A., Andreeva, N. S., and James, M. N. (1990) Molecular and crystal structures of monoclinic porcine pepsin refined at 1.8 A resolution, *J. Mol. Biol. 214*, 143−170.
40. Dreyer, G. B., Metcalf, B. W., Tomaszek, T. A., Jr., Carr, T. J., Chandler, A. C., III, Hyland, L., Fakhoury, S. A., Magaard, V. W., Moore, M. L., Strickler, J. E., and et al. (1989) Inhibition of human immunodeficiency virus 1 protease in vitro: rational design of substrate analogue inhibitors, *Proc. Natl. Acad. Sci. U.S.A. 86*, 9752−9756.
41. Piana, S., and Carloni, P. (2000) Conformational flexibility of the catalytic Asp dyad in HIV-1 protease: An ab initio study on the free enzyme, *Proteins 39*, 26−36.
42. Northrop, D. B. (2001) Follow the Protons: A Low-Barrier Hydrogen Bond Unifies the Mechanisms of the Aspartic Proteases, *Acc. Chem. Res. 34*, 790−797.
43. Dunn, B. M. (2002) Structure and mechanism of the pepsin-like family of aspartic peptidases, *Chem. Rev. 102*, 4431−4458.
44. Coates, L., Erskine, P. T., Wood, S. P., Myles, D. A. A., and Cooper, J. B. (2001) A Neutron Laue Diffraction Study of

Endothiapepsin: Implications for the Aspartic Proteinase Mechanism, *Biochemistry 40*, 13149−13157.
45. Das, A., Prashar, V., Mahale, S., Serre, L., Ferrer, J. L., and Hosur, M. V. (2006) Crystal structure of HIV-1 protease in situ product complex and observation of a low-barrier hydrogen bond between catalytic aspartates, *Proc. Natl. Acad. Sci. U.S.A. 103*, 18464−18469.
46. Trylska, J., Grochowski, P., and McCammon, J. A. (2004) The role of hydrogen bonding in the enzymatic reaction catalyzed by HIV-1 protease, *Protein Sci. 13*, 513−528.
47. Frey, P. A. (2001) Strong hydrogen bonding in molecules and enzymatic complexes, *Magn. Reson. Chem. 39*, S190−S198.
48. Cleland, W. W., Frey, P. A., and Gerlt, J. A. (1998) The low barrier hydrogen bond in enzymatic catalysis, *J. Biol. Chem. 273*, 25529−25532.
49. Cleland, W. W., and Kreevoy, M. M. (1994) Low-barrier hydrogen bonds and enzymic catalysis, *Science 264*, 1887−1890.
50. Gelb, M. H., Svaren, J. P., and Abeles, R. H. (1985) Fluoro ketone inhibitors of hydrolytic enzymes, *Biochemistry 24*, 1813−1817.
51. James, M. N. G., Sielecki, A. R., Hayakawi, K., and Gelb, M. H. (1992) Crystallographic Analysis of Transition State Mimics Bound to Penicillopepsin Difluorostatine- and Difluorostatone-Containing Peptides, *Biochemistry 31*, 3872−3886.
52. Fersht, A. R. (1987) The hydrogen bond in molecular recognition, *Trends Biochem. Sci. 12*, 301−304.
53. Bachovchin, W. W. (1985) Confirmation of the assignment of the low-field proton resonance of serine proteases by using specifically nitrogen-15 labeled enzyme, *Proc. Natl. Acad. Sci. U.S.A. 82*, 7948−7951.
54. Bao, D., Chen, J. T., Kettner, C., and Jordan, F. (1998) Assignment of the $N^{\varepsilon 2}$ and $N^{\delta 1}$ Resonances at the Active-Center Histidine in Chymotrypsin and Subtilisin Complexed to Peptideboronic Acids without Specific ^{15}N Labelling, *J. Am Chem. Soc. 120*, 3485−3489.
55. Robillard, G., and Shulman, R. G. (1974) High Resolution Nuclear Magnetic Resonance Studies of the Active Site of Chymotrypsin, *J. Mol. Biol. 86*, 519−540.

BI701000K